Range Extension Autonomous Driving for Electric Vehicles Based on Optimal Velocity Trajectory and Driving Braking Force Distribution Considering Road Gradient Information

Hideki Yoshida
Hiroshi Fujimoto
The University of Tokyo
5-1-5, Kashiwanoha, Kashiwa, Chiba, 27 7-8561 Japan
Telephone: +81-4-7136-3881
Fax: +81-4-7136-3881
Email: yoshida14@hflab.k.u-tokyo.ac.jp
fujimoto@k.u-tokyo.ac.jp

Daisuke Kawano
Yuichi Goto
National Traffic Safety
and Environment Laboratory
7-42-27, Jindaijihigashimachi,
Chofu, Tokyo, 182-0012 Japan
Phone: +81-422-41-3207
Email: kawano@ntsel.go.jp,
goto@ntsel.go.jp

Misaki Tsuchimoto
Koji Sato
Ono Sokki Co., Ltd.
3-9-3, Shin-Yokohama, Kohoku-ku,
Yokohama, Kanagawa, 222-8507 Japan
Phone: +81-45-935-3872
Email: mtsuchim@onosokki.co.jp,
satoko@onosokki.co.jp

***Abstract*—Electric Vehicles (EVs) are deemed as an appealing and practical solution for environmental and energy problems. The mileage per charge of EVs, however, is shorter than the mileage of Internal Combustion Engine Vehicles (ICEVs). In this paper, Range Extension Autonomous Driving (READ) system considering road gradient information is proposed. The proposed system optimizes the velocity trajectory and the driving–braking force distribution ratio for autonomous driving. The authors carried out simulations and bench tests that prove the effectiveness of the proposal in terms of mileage per charge.**

I. Introduction

Recently Electric Vehicles (EVs) have been noted to be a solution to the current environmental and energy problems. In addition, EVs have novel advantages over Internal Combustion Engine Vehicles (ICEVs): the three main advantages are listed as below.

1) The response of torque by motor is much faster than that of engines (100 times) .
2) In–wheel motors enable independent driving force control.
3) Motor torque can be measured precisely from the motor current.

These advantages are demonstrated to be useful for motion control of EVs [1], [2].

However, the short mileage per charge of EVs prevents them to be widespread. In order to solve this problem, lots of methods were proposed. For example, a control system was proposed to reduce iron loss by regulating the flux density of motors [3]. Any other research works considered the optimization of driving force distribution in terms of motor efficiency [4]–[7]. However, these studies assumed that driver decides vehicle velocity and did not consider minimizing the total energy consumption.

Fig. 1: FPEV2–Kanon on RC–S Bench.

The Intelligent Transport Systems (ITS) are capable of two–way communication between transportation infrastructure and vehicle. So we consider that vehicle will control vehicle velocity in the near future.

The authors' research group has proposed Range Extension Control Systems (RECS) [6] and Range Extension Autonomous Driving (READ)[8]–[9]. These methods extends mileage per charge using only motion control techniques which do not change motor type or vehicle structures. RECS optimizes the driving force distribution. On the other hand, READ optimizes the velocity trajectory and the driving force distribution. Assuming that road gradient information is available from on board devices such as Global Positioning System (GPS), conventional READ can reduce more energy consumption considering road gradient information [8]. However, important factors such as driving–braking force distribution are not being considered.

In this study, the velocity trajectory and driving–braking force distribution are designed by formulating an optimization algorithm. The effectiveness of proposed method is verified by simulations and experiments.

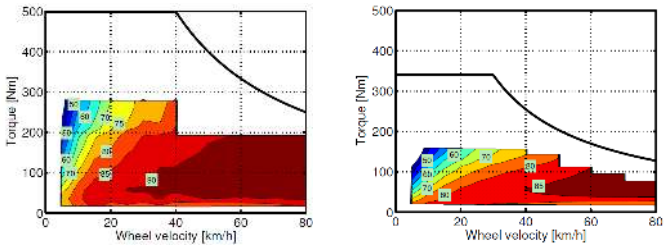

(a) Front motor. (b) Rear motor.

Fig. 2: Efficiency maps of front and rear motors.

TABLE I: Vehicle specification.

Meaning	Symbol	Value
Vehicle mass	M	854 kg
Wheel base	l	1.72 m
Distance from CG to front axle	l_f	l_f : 1.01 m
Distance from CG to rear axle	l_r	l_r : 0.702 m
Front wheel inertia	$J_{\omega f}$	1.24 kgm^2
Rear wheel inertia	$J_{\omega r}$	1.26 kgm^2
Wheel radius	r	0.302 m

TABLE II: Specifications of in–wheel motors.

	Front	Rear
Manufacturer	TOYO DENKI SEIZO K.K.	
Type	Direct drive system Outer rotor type	
Rated torque	110 Nm	137 Nm
Maximum torque	500 Nm	340 Nm
Rated power	6.00 kW	4.30 kW
Maximum power	20.0 kW	10.7 kW
Rated speed	382 rpm	300 rpm
Maximum speed	1110 rpm	1500 rpm

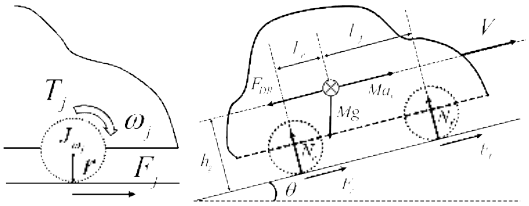

(a) Rotational motion of a wheel. (b) Load transfer model.

Fig. 3: Vehicle model.

II. Experimental Vehicle and Model

A. Experimental Vehicle

In this research, an original electric vehicle "FPEV2–Kanon" manufactured by the authors' research group is used. The picture and the specification of the vehicle are shown in Fig. 1 and Tab. I. This vehicle has four outer–rotor type in–wheel motors. These motors are direct drive type. Therefore the reaction forces from the road are directly transferred to the motor without the backlash influence of the reduction gear. Tab. II shows the specification of the motors. Fig 2 shows efficiency maps of the front and the rear in–wheel motors. Lithium-ion battery is used as power source. The voltage of the main battery is 160 V. The voltage is boosted to 320 V by a converter. In this paper, the converter loss is neglected.

B. Vehicle Model

In this section, a four wheel driven vehicle model is described. Using the model given in Fig. 3(a), the wheel dynamics is expressed as Eq.(1). From Fig. 3(b), the vehicle dynamics are expressed as Eq.(2)–(4)

$$J_{\omega_j}\dot{\omega}_j = T_j - rF_j, \tag{1}$$

$$M\dot{V} = F_{\rm all} - {\rm sgn}(V)F_{\rm DR}(V,\theta) - Mg\sin\theta, \tag{2}$$

$$F_{all} = 2\sum_{j=f,r} F_j, \tag{3}$$

$$F_{\rm DR}(V,\theta) = \mu_0 Mg\cos\theta + b|V| + \frac{1}{2}\rho C_{\rm d} A V^2, \tag{4}$$

where ω_j is the wheel angular velocity, V is the vehicle velocity, T_j is the motor torque, F_j is the driving force of each wheel, $F_{\rm all}$ is the total driving force, M is the vehicle mass, r is the wheel radius, J_{ω_j} is the wheel inertia, $F_{\rm DR}$ is the driving resistance, μ_0 is rolling friction coefficient, θ is road gradient, b is resistance vehicle velocity coefficient, ρ is air density, $C_{\rm d}$ is constant drag and A is frontal projected area. The subscript j represents f or r, f stands for "front" and r represents "rear".

The slip ratio λ_j is defined as

$$\lambda_j = \frac{V_{\omega_j} - V}{\max(V_{\omega_j}, V, \epsilon)}, \tag{5}$$

where $V_{\omega_j} = r\omega_j$ is the wheel speed and ϵ is a small constant to avoid zero division. The slip ratio λ_j is known to be related with the friction coefficient μ_j [10]. In the region $|\lambda_j| \ll 1$, μ_j is nearly proportional to λ_j. Then, for longitudinal acceleration cases,

$$F_j = \mu_j N_j \approx D_s{}' N_j \lambda_j, \tag{6}$$

where $D_s{}'$ is the normalized driving stiffness.

The normal forces of each wheel during the longitudinal acceleration process are calculated as follows

$$N_f(\dot{V},\theta) = \frac{1}{2}\left[\frac{l_r}{l}Mg\cos\theta - \frac{h_g}{l}M\dot{V}\right], \tag{7}$$

$$N_r(\dot{V},\theta) = \frac{1}{2}\left[\frac{l_f}{l}Mg\cos\theta + \frac{h_g}{l}M\dot{V}\right], \tag{8}$$

where N_f and N_r are respectively the front and rear normal forces, l_f and l_r are respectively the distances from the center of gravity to the front and rear axles, l is the wheelbase, and h_g is the height of the center of gravity. The acceleration direction is defined as positive when the vehicle is accelerating.

C. Driving–Braking Force Distribution [6]

During straight driving, the required total driving–braking force can be distributed to each wheel. Since the EV motors were assumed to be independently controlled in this study, the driving–braking force distribution has an extra degree of

freedom. By introducing the front and rear driving–braking force distribution ratio k, the driving–braking forces can be formulated based on the total driving–braking force $F_{\rm all}$ and the distribution ratio k as follows

$$F_j = \frac{1}{2}\gamma_j(k)\,F_{\rm all}, \tag{9}$$

$$\gamma_j(k) = \begin{cases} 1-k & (j=f) \\ k & (j=r) \end{cases}. \tag{10}$$

The distribution ratio k varies from 0 to 1. $k=0$ means that the vehicle is a front–driven system, and $k=1$ means that it is rear–driven system.

D. Power Flow Model [6]

The inverter input power $P_{\rm in}$ considering the slip ratio and motor loss is expressed as

$$P_{\rm in} = P_{\rm out} + P_{\rm c} + P_{\rm i}, \tag{11}$$

where $P_{\rm out}$ is the sum of the mechanical output of each motor, $P_{\rm c}$ is the sum of the copper loss of each motor, and $P_{\rm i}$ is the sum of the iron loss of each motor. The inverter loss and mechanical loss are neglected. When each wheel angular acceleration is small, torque T_j is proportional to driving force. T_j is expressed as

$$T_j \approx rF_j. \tag{12}$$

When the slip ratioλ_j is small enough, ω_j is expressed as

$$\omega_j = \frac{V}{r(1-\lambda_j)} \approx \frac{V}{r}(1+\lambda_j). \tag{13}$$

By substituting Eq.(6) in Eq.(9), λ_j is expressed as

$$\lambda_j = \frac{F_j}{{D_s}' N_j(\dot{V},\theta)} = \frac{\gamma_j(k)\,F_{\rm all}}{2{D_s}' N_j(\dot{V},\theta)}. \tag{14}$$

Approximated $P_{\rm out}$, $P_{\rm c}$ and $P_{\rm i}$ are expressed as

$$P_{\rm out} = 2\sum_{j=fr}\omega_j T_j \simeq V\frac{F_{\rm all}}{2}\sum_{j=f,r}\left(1+\frac{\gamma_j(k)\,F_{\rm all}}{2{D_s}' N_j(\dot{V},\theta)}\right), \tag{15}$$

$$P_{\rm c} = 2\sum_{j=f,r} R_j {i_{qj}}^2 = \frac{r^2}{2}{F_{\rm all}}^2\sum_{j=f,r}\frac{R_j}{{K_{tj}}^2}{\gamma_j}^2(k), \tag{16}$$

$$P_{\rm i} = \frac{2V^2}{r^2}\sum_{j=f,r}\frac{{P_{nj}}^2}{R_{cj}}\left[\left(\frac{rL_{qj}\gamma_j(k)\,F_{\rm all}}{2K_{tj}}\right)^2 + {\Psi_j}^2\right], \tag{17}$$

where R_j is the armature winding resistance of the motor, K_{tj} is the torque coefficient of the motor, P_{nj} is the number of pole pairs, L_{qj} is the q–axis inductance and Ψ_j is the interlinkage magnetic flux.

The electrical angular velocity of the motor ω_{ej} and the equivalent iron loss resistance R_{cj} are expressed as

$$\omega_{ej} = \frac{P_{nj}V}{r}, \tag{18}$$

$$\frac{1}{R_{cj}} = \frac{1}{R_{c0j}} + \frac{1}{{R_{c1j}}'|\omega_{ej}|}, \tag{19}$$

where the first and second terms on the right–hand side represent the eddy current loss and hysteresis loss, respectively.

The road gradient can be estimated from the distance traveled on condition that grade map data is stored in advance. Therefore, the road gradient function θ can be described by the distance traveled X. Then the inverter input power is expressed by V, X and $F_{\rm all}$ as

$$\theta = \theta(X) \tag{20}$$

$$P_{\rm in}(V,X,F_{\rm all},k) = P_{\rm out}(V,X,F_{\rm all},k) + P_{\rm c}(F_{\rm all},k) + P_{\rm i}(V,F_{\rm all},k) \tag{21}$$

III. Optimization of Velocity Trajectory Considering Road Gradient Information

A. The Evaluation Function and the Constraint Conditions

In this section, under assumption of autonomous driving, we propose READ which calculates optimal velocity trajectory minimizing the total amount of energy consumption from initial time t_0 to final time t_f. EVs can regenerate kinematic energy. Therefore, minimization of total energy consumption is equal to maximization of regenerative energy. The evaluation function and the constraint conditions are described as

$$\text{min. } W_{\rm in} = \int_{t_0}^{t_f} P_{\rm in}(\boldsymbol{x}(t),\boldsymbol{u}(t))dt, \tag{22}$$

$$s.t.\ \dot{\boldsymbol{x}}(t) = \boldsymbol{f}(\boldsymbol{x}(t),\boldsymbol{u}(t)), \tag{23}$$

$$\chi(\boldsymbol{x}(t_0)) = \boldsymbol{x}(t_0) - \boldsymbol{x}_0 = \boldsymbol{0}, \tag{24}$$

$$\psi(\boldsymbol{x}(t_f)) = \boldsymbol{x}(t_f) - \boldsymbol{x}_f = \boldsymbol{0}, \tag{25}$$

$$\boldsymbol{x}(t) = \begin{bmatrix} V(t) \\ X(t) \end{bmatrix}, \boldsymbol{u}(t) = \begin{bmatrix} F_{\rm all}(t) \\ k(t) \end{bmatrix}, \tag{26}$$

where $X(t)$ is the distance traveled and $\boldsymbol{x_0}$ is the initial condition of velocity and distance traveled. $\boldsymbol{x_f}$ is the final condition of velocity and distance traveled.

Optimal velocity trajectory and driving–braking force distribution ratio to minimize the total amount of energy consumption are derived by solving this optimal control problem. Since $P_{\rm in}$ is a quadratic function of k, optimal distribution ratio $k_{\rm opt}$ which minimizes $P_{\rm in}$ satisfies $\dfrac{\partial P_{\rm in}}{\partial k} = 0$. Therefore, $k_{\rm opt}$ is derived as a function of V ,$F_{\rm all}$ and $\theta(X)$ as known:

$$k_{\rm opt}\ (V,F_{\rm all},\theta(X)) = \frac{\frac{V}{{D_s}' N_f(V,F_{\rm all},\theta(X))} + \frac{r^2R_f}{{K_{tf}}^2} + \frac{V^2}{R_{cf}}\left(\frac{L_{qf}}{\Psi_f}\right)^2}{\frac{V}{{D_s}'}\sum_{j=f,r}\frac{1}{N_j(V,F_{\rm all},\theta(X))} + r^2\sum_{j=f,r}\frac{R_j}{{K_{tj}}^2} + V^2\sum_{j=f,r}\frac{1}{R_{cj}}\left(\frac{L_{qj}}{\Psi_j}\right)^2} \tag{27}$$

By applying $k_{\rm opt}$ at all times, this problem becomes one dimensional search. In this paper, steepest descent method is used to calculate vehicle velocity trajectory.

B. Comparison Conditions

We assume that the vehicle runs at V_0 by the starting point X_0 and will stop with V_f at the goal X_f. In this paper, six cases are considered. Three types of trajectories are calculated under each distribution ratio which is $k = 0.5, k_{\rm opt}$. In this

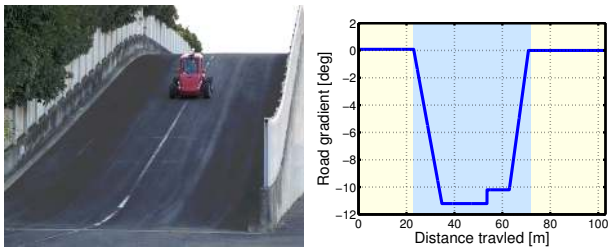

(a) Assumed test road. (b) Road gradient profile.

Fig. 4: Assumed test road and road gradient profile.

TABLE III: Driving resistance condition

Meaning	Symbol	Value
Rolling friction coefficients	μ_0	1.28×10^{-2}
Constant drag	C_d	0.806
Frontal projected area	A	1.20 m^2
Driving stiffness	$D_s{}'$ (dry asphalt)	12.0

section, the velocity trajectories are explained to compare with proposed velocity trajectory.

Trajectory 1 Constant Deceleration

Trajectory 1 is a conventional method assuming that a driver stops after constant deceleration. The velocity trajectory $V(t)$ and final time t_f are described as

$$V(t) = V_0 + \frac{{V_f}^2 - {V_0}^2}{2(X_f - X_0)}(t - t_0), \quad (28)$$

$$t_f = \frac{2(X_f - X_0)}{V_f + V_0} + t_0, \quad (29)$$

where V_0 is initial velocity and X_f is final distance traveled.

Trajectory 2 Optimized Velocity Trajectory Not Considering Road Gradient Information

Trajectory 2 is a conventional method which minimizes energy consumption by autonomous driving, but without considering road gradient. Then road gradient is assumed as $\theta(X) = 0$.

Trajectory 3 Optimized Velocity Trajectory Considering Road Gradient Information

Trajectory 3 is a proposed method which minimizes energy consumption by autonomous driving, considering road gradient.

IV. Simulation

A. Simulation Conditions

Fig. 4(a) shows the test road at National Traffic Safety and Environment Laboratory. Fig. 4(b) illustrates the road gradient profile of the test road. The simulation conditions are given in Table III. The initial condition is given as t_0=0.00 s, V_0=30.0 km/h, X_0=0.00 m. The final condition is given as V_f=0.00 km/h, X_f=103 m. t_f is 24.7 s which is calculated from Eq.29.

B. Control System

Vehicle velocity control system is designed to control the EVs velocity automatically. Fig. 5 shows the system which is

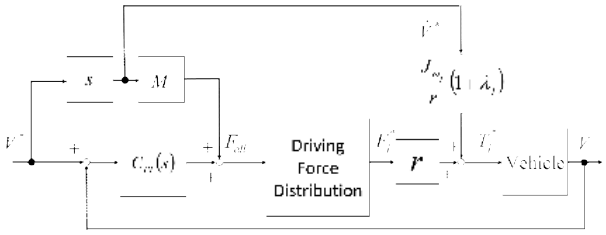

Fig. 5: Vehicle velocity control system.

composed of a feedforward controller and feedback controller. Front and rear torque reference $T_j{}^*$ is given as

$$T_j{}^* = rF_j{}^* + \frac{J_{\omega_j}\dot{V}^*}{r}(1+\lambda_j). \quad (30)$$

The second term of right hand side compensates inertia of the wheels. Vehicle velocity controller $C_{PI}(s)$ is a PI controller, and it is designed by the pole placement method. The plant of vehicle velocity is expressed as

$$\frac{V}{F_{\mathrm{all}}} = \frac{1}{Ms}. \quad (31)$$

In the simulations and the experiments, the poles of vehicle velocity controller are set to -5 rad/s.

C. Simulation Results

Fig. 6 and Table IV show simulation results on 6 cases. Light blue section shows the downward slope. In this paper, case (A), (C), (E) are treated as conventional trajectory 1, 2 and 3, respectively. Case (F) is the proposed trajectory. Fig. 6(d)–Fig. 6(g) show the dominant loss of power flow model.

To analyze the simulation results, mechanical output P_{out} is separated into the power stored as kinetic energy of vehicle mass P_{M}, the sum of the power stored as rotational energy of each wheel P_{J}, the loss caused by the driving resistance P_{R}, and the sum of the loss caused by slip of each wheel P_{S}. The integrated values of these values are described as

$$W_{\mathrm{X}} = \int_{t_0}^{t_f} P_{\mathrm{X}}(\boldsymbol{x}(t), \boldsymbol{u}(t))dt, \quad (32)$$

where the subscript X represents “out”, “M”, “J”, “R”, “S”, “c”, and “i” as explained previously.

When vehicle reduces in the speed on the downward slope, motors can convert potential energy and kinematic energy to electric energy. In case (A), motors must generate larger total braking force than road gradient resistance to reduces in the speed at a constant deceleration on the downward slope. Therefore copper loss becomes large and regenerative energy becomes small. In case (E), when the vehicle runs on the flat area from 0.00 to 23.0 m, vehicle reduces speed more quickly than case (A) to prevent losing kinematic energy by driving resistance. Then regenerative energy of case (E) is larger than that of case (A). When the vehicle runs on the downward slope from 23.0 to 60.0 m, deceleration of case (E) is larger than that of case (A). Then copper loss of case (E) is slightly bit larger than that of case (A). In case (C), on the flat area, the vehicle reduces in speed at an optimal deceleration to prevent

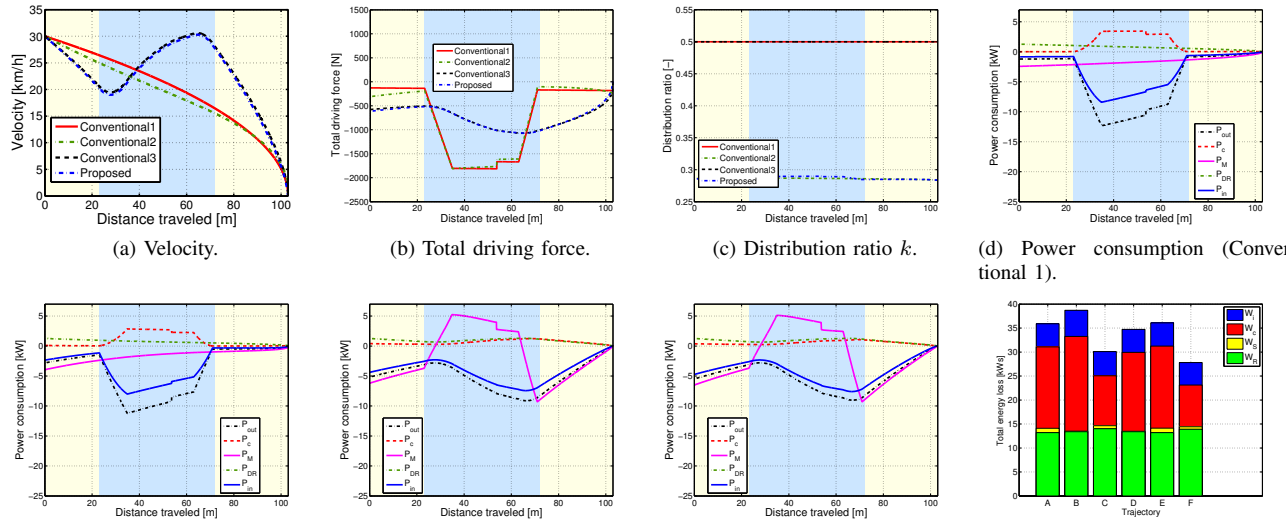

(a) Velocity. (b) Total driving force. (c) Distribution ratio k. (d) Power consumption (Conventional 1).

(e) Power consumption (Conventional 2). (f) Power consumption (Conventional 3). (g) Power consumption (Proposed). (h) Energy loss.

Fig. 6: Simulation results of pattern driving.

TABLE IV: Regenerative energy [kWs](Simulation result).

k	Trajectory 1	Trajectory 2	Trajectory 3
0.5	53.7 (A) Conventional 1	52.5 (B)	62.4 (C) Conventional 3
k_{opt}	57.6 (D)	55.8 (E) Conventional 2	64.4 (F) Proposed

the vehicle from losing kinematic energy by driving resistance. On the other hand, copper loss is larger than that of both case (A) and (E). On the downward slope, the vehicle reduces in speed at an optimal acceleration to suppress the copper loss. If vehicle runs at deceleration such as case (A) or (E), the driving force causes large copper loss on the downward slope. On the other hand, if vehicle accelerates with a larger Value than that of case (C) or (F) on the downward slope, driving force becomes larger than that of case (C) or (F) on the down flat area and cause large copper loss on the down flat area. Therefore optimal velocity trajectory is defined by the trade off between copper loss on the down flat area and that on the downward area. Inverter input power of case (C) is larger than that of both case (A) and (E) to suppress copper loss on the flat area. In case (F), optimization of driving–braking force distribution suppress more copper loss than that of other cases on the all area.

As shown in Table IV, regenerative energy of case (A), (C), (E), (F) are 53.7 kWs, 62.4 kWs, 55.8 kWs, and 64.4 kWs, respectively. Regenerative energy of proposed case (F) improved 23.5 %, 24.5 %, 7.75 % compared with that of conventional case (A), (E), (C). Therefore, the algorithm to maximize regenerative energy should be designed in consideration of two cases: 1) Reduce regenerative braking if it increases the copper loss: 2) Increase regenerative braking in the case it has little influence on the copper loss, i.e., hard braking can reduce driving resistance loss.

V. Experiment

Experiments were conducted on the Real Car Simulation Bench (RC–S)[11] shown in Fig. 1 under the same condition as simulations. RC-S owned by ONO Sokki Co., Ltd. can reproduce various travel situation without being influenced by change of wind and road surface condition.

Vehicle velocity V, inverter input power P_{in}, mechanical output P_{out}, total loss P_{L} including motor copper loss , motor iron loss and inverter loss, and driving resistance loss P_{R} are calculated as

$$V = \frac{r}{4}\sum_{j=f,r}\sum_{i=l,r}\omega_{ij}, \tag{33}$$

$$P_{\mathrm{in}} = V_{\mathrm{dc}}\sum_{j=f,r} I_{\mathrm{dc}j}, \tag{34}$$

$$P_{\mathrm{out}} = \sum_{i=l,r}\sum_{j=f,r}\omega_{ij}T_{ij}, \tag{35}$$

$$P_{\mathrm{L}} = P_{\mathrm{in}} - P_{\mathrm{out}}, \tag{36}$$

$$P_{\mathrm{R}} = F_{\mathrm{DR}}V = (\mu_0 Mg\cos\theta + b|V| + \frac{1}{2}\rho C_{\mathrm{d}}AV^2)V, \tag{37}$$

where the subscript i represents l or r (l stands for left and r represents right wheel). V_{dc} is measured the inverter input voltage and $I_{\mathrm{dc}j}$ is the measured inverter input current. P_{in} includes inverter loss.

Fig. 7 shows experimental results which are the average values and standard deviations of the experiments repeated five times. Table V shows regenerative energy. Average regenerative energy of case (A), (C), (E), (F) is 53.2 kWs, 55.6 kWs, 61.0 kWs and 65.7 kWs respectively. Average regenerative energy of proposed case (F) improved significantly 23.5 %, 24.5 %, 7.75 % compared with that of conventional case

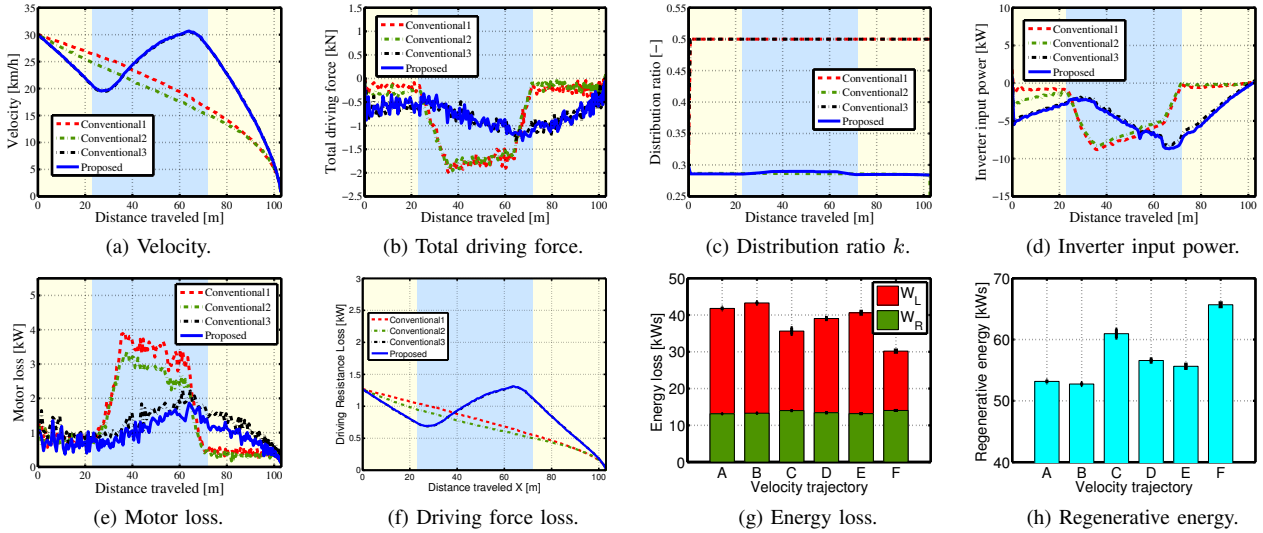

(a) Velocity. (b) Total driving force. (c) Distribution ratio k. (d) Inverter input power.

(e) Motor loss. (f) Driving force loss. (g) Energy loss. (h) Regenerative energy.

Fig. 7: Experimental results of pattern driving.

TABLE V: Regenerative energy [kWs](Experimental result: Average±Standard deviation).

k	Trajectory 1	Trajectory 2	Trajectory 3
0.5	53.2±0.294 (A) Conventional 1	52.7±0.251 (B)	61.0±0.729 (C) Conventional 3
k_{opt}	56.6±0.280 (D)	55.6±0.358 (E) Conventional 2	65.7±0.329 (F) Proposed

(A), (C), (E). The experimental results are consistent with simulation results.

VI. Conclusion

This paper proposed a READ system that can optimally generate vehicle velocity and driving braking force distribution to reduce energy consumption considering road gradient information. In the experiments, it is demonstrated that the proposed method increases regenerative energy by 7.75 % in comparison with the conventional READ systems.

The future works include: 1) Consider constraints on speed and acceleration on general roads and highways, 2) Consider the space between a car and the one in front.

Acknowledgment

This research was partly supported by Industrial Technology Research Grant Program from New Energy and Industrial Technology Development Organization (NEDO) of Japan (number 05A48701d), and by the Ministry of Education, Culture, Sports, Science and Technology grant (number 22246057 and 26249061).

References

[1] Y. Hori: "Future Vehicle Driven by Electricity and Control–Research on Four–Wheel–Motored" UOT Electric March II"," IEEE Trans. on Industrial Electronics, Vol. 51, No. 5, pp.954–962 (2004).

[2] K. Maeda H. Fujimoto and Y. Hori: "Four–wheel Driving–force Distribution Method for Instantaneous or Split Slippery Roads for Electric Vehicle" Automatika – Journal for Control Measurement Electronics Computing and Communications pp. 103–113 (2013).

[3] H. Hijikata, K. Akatsu, Y. Miyama, H Arita, and A. Daikoku: "Suppression Control Method for Iron Loss of MATRIX Motor under Flux Weakening Utilizing Individual Winding Current Control,"The 7th International Power Electronics Conference, IPEC–Hiroshima 2014 - ECCE Asia-, pp. 2673–2678 (2014).

[4] Y. P. Yang, Y. C. Shih, and J. M. Chen: "Real–Time Distribution Strategy for an Electric Vehicle with Multiple Traction Motors by Particles Swarm Optimization," CACS International Automatic Control Conference, pp. 233–238 (2013).

[5] S. Egami and H. Fujimoto: "Range Extension Control System for Electric Vehicle Based on Front and Rear Driving Force Distribution Considering Load Transfer" in Proc. 37th Annual Conference of the IEEE Industrial Electronics Society Melbourne pp.3721–3726 (2011).

[6] H. Fujimoto and S. Harada: "Model–Based Range Extension Control System for Electric Vehicles With Front and Rear Driving–Braking Force Distributions,"IEEE Trans. on Industrial Electronics, Vol. 62, No. 5, pp. 3245–3254 (2015).

[7] X. Yuan, J. Wang, and K. Colombage: "TORQUE DISTRIBUTION STRATEGY FOR A FRONT AND REAR WHEEL DRIVEN ELECTRIC VEHICLE," IEEE Trans. on Vehicular Technology, Vol. 61, No. 8, pp. 3365–3374 (2012).

[8] H. Yoshida and H. Fujimoto: "Range Extension Autonomous Driving for Electric Vehicles Based on an Optimal Vehicle Velocity Trajectory Considering Road Gradient Information," The 1st IEEJ International Workshop on Sensing Actuation and Motion Control , pp. 1 –6 (2015).

[9] Y. Ikezawa, H. Fujimoto, and Y. Hori: "Range Extension Autonomous Driving for Electric Vehicles Based on Optimal Vehicle Velocity Trajectory Generation and Front–Rear Driving–Braking Force Distribution with Time Constraint," The 1st IEEJ International Workshop on Sensing Actuation and Motion Control , pp. 1 –6 (2015).

[10] H. B. Pacejka and E. Bakker: "The Magic Formula Tyre Model," Vehicle System Dynamics, International Journal of Vehicle Mechanics and Mobility, Vol. 21, No. 1, pp. 1–18 (1992).

[11] D. Kawano, Y. Goto, K. Echigo, and K. Sato: "Analysis of Behavior of Fuel Consumption and Exhaust Emissions under On–road Driving Conditions Using Real Car Simulation Bench (RC–S)," 2009 JSAE Annual Congress (Spring) Vol. 19, pp. 9–12 (2009) (in Japanese).